Sigma J Eng & Nat Sci 38 (3), 2020, 1427-1445

Sigma Journal of Engineering and Natural Sciences
Sigma Mühendislik ve Fen Bilimleri Dergisi

Research Article

CYCLIC BEHAVIOR OF COMPOSITE COLUMN-REINFORCED CONCRETE BEAM JOINTS

Fethi ŞERMET[1], Emre ERCAN[2], Emin HÖKELEKLİ[3], Bengi ARISOY*[4]

[1]*Iğdır University, Civil Engineering Department, IĞDIR;* ORCID: 0000-0001-8221-689X
[2]*Ege University, Civil Engineering Department, İZMİR;* ORCID: 0000-0001-9325-8534
[3]*Bartın University, Civil Engineering Department, BARTIN;* ORCID: 0000-0003-0548-5214
[4]*Ege University, Civil Engineering Department, İZMİR;* ORCID: 0000-0002-2785-0609

Received: 31.12.2019 Revised: 11.05.2020 Accepted: 13.06.2020

ABSTRACT

In this paper, behavior of the concrete encased steel profile composite column-reinforced concrete beam connection representing interior beam-to-column joints under cyclic loading is presented. The column was designed as concrete encased I steel profile composite column according to Eurocode 4; beam was designed as regular reinforced concrete beam according to local building codes. The finite element model of the beam-to-column joint was implemented in ABAQUS and numerical analysis was validated by full scale experimental study. The performance of the concrete encased steel profile composite column-reinforced concrete beam joint was compared to reinforced concrete beam-to-column joint, in order to observe the load carrying capacity and ductility. Ductility level and failure type of the joints were studied and performance of connections are compared. Comparisons were made using load-displacement relation and failure mechanism. It is found that the concrete encased steel composite column-reinforced concrete beam joint exhibited slightly ductile behavior relative to reinforced concrete column-beam joint. On the other hand, analysis result show that the failure controlled by behavior of the beam and joint capacity is depend on the shear capacity of the beam.

Keywords: Reinforced concrete joints, composite columns, cyclic loading, finite element modeling.

1. INTRODUCTION

In reinforced concrete moment resisting frames, joints are designed as rigid connection and it is expected that the joints allow the members (beams and columns) adjoining in joint to develop and sustain their ultimate capacity. Under seismic loading, the demand of ductile behavior of the joint is increased and adequate strength and stiffness of the joint to resist the internal forces induced by the framing members should be provided. On the other hand, the beam-to-column joints are the most critical sections in the reinforced concrete frame systems under seismic loading. In earthquake resistant building design, it is intended that the beam-to-column joints are to consume the earthquake loads by deformations. In this approach, the ductility of the structure is one of the most important parameters. A ductile structure maintains its strength in spite of the fact that the elements make plastic deformations under the effect of earthquake loads. In order to

* Corresponding Author: e-mail: bengi.arisoy@ege.edu.tr, tel: (232) 311 51 81

maintain enough ductility of the frame system, especially in joint sections, different applications are engineered. The structural frames generated using concrete encased steel profile composite members are one of the engineered applications. The reinforced concrete beam-to-column joints already exhibits complex behavior under bending, shear and axial load combinations. When the complexity of the members in joint section is increased, the complexity of the behavior is increased natur ally. Using composite column in beam-to-column joint causes more complex behavior due to by the fact that members that connect at joint have different properties. Although studies on determining the behavior of concrete encased steel profile composite members (columns and beams, individually) under cyclic load were started in the 1940s, the studies on beam-to-column joints are newer.

The studies performed on composite column-composite slab/composite beam connections indicate that the composite columns are far strong than adjoining horizontal members, the failure always occurs in horizontal members without any failure in composite column unless the failure of the column is persuaded [1-12]. The studies performed on composite column-steel beams exhibit that in this case, the concrete cover around steel profile in composite columns are crushed without reaching expected performance [13-15]. The analytical studies about behavior of the joint section of concrete encased steel profile members are relatively limited; on the other hand, wide ranges of numerical studies exist about the subject [16-20].

In this study, behavior of an engineered beam-to-column joint, consist of concrete encased steel profile column and reinforced concrete beam joint (SAMPLE 1) and concrete reinforced concrete beam-column joint (SAMPLE 2), given in Fig. 1-a and b, respectively, were experimentally and numerically studied. SAMPLE 1 was a sample represented the commercial applications widely used in high-rise buildings in Turkey. This design has been used because of "strong column-weaker beam" design regulation is guaranteed with smaller cross section that is much economical than reinforced concrete column with same capacity. On the other hand, although concrete encased steel composite column was proved itself being high ductility, it should be studied that this ductility is still valid when certain joint under loading. SAMPLE 2 was a sample presents the regular reinforced concrete beam-column joint full fill the building codes required. Thus, it would be studied if the joint as in SAMPLE 1 satisfy the expectations.

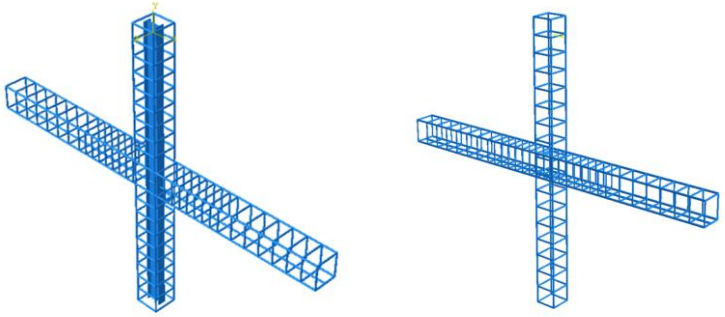

(a) Concrete encased steel profile column and reinforced concrete beam (SAMPLE 1)

(b) Reinforced concrete beam-column (SAMPLE 2)

Figure 1. Model of the specimens

In this matter, two large scale samples were prepared and tested, and a Finite Element (FE) model was implemented into ABAQUS [21], to gather stress distribution of the section, deformation of the joint, moment-curvature relation for beam and column parts of the connection and predict failure modes of the joint under axial compressive and horizontal cyclic loading. The

concrete damage plasticity (CDP), surfa ce contact modeling, meshing principles are included to the FE modeling of the joint in order to complete the modeling. The analysis results were compared in order to exhibit the performance of the engineered beam-to-column joints.

2. SIGNIFICANCE OF THE STUDY

In the earthquake resistant moment frame design, it is expected that the energy built up in the joint due to earthquake loads are spend by deformations. The most important parameter in this approach is the ductility of the structure. A ductile structure maintains its strength even though its members undergo plastic deformations under the effect of earthquake loads. The concrete encased steel profile composite columns are satisfy both strength and ductility capacity under seismic loads [24-28]. Therewith, the beam connected to the composite column is designed as reinforced concrete beam, thus, the strong column-weaker beam design is satisfied, and thus the plastic hinges would occur in beams. On the other hand, behavior of the beam-to-column joint is controlled by the bond between steel and concrete, and the shear strength of the joint, so that, the capacity of the joint depends on the capacity of the beam. This study would provide the verification whether the engineered joint design supplies expected capacity. In this study, the beam-to-column joints proposed above were analyzed both experimentally and numerically to understand whether the joint satisfied the properties expected. In addition to that, the strength capacity and ductility level of the joint were identified; failure mechanism of the connection was defined.

The joint studied is an interior beam-to-column connection (Fig. 2). The dimensions of the members to be modeled are determined by taking advantage of the moment zero points of the frame affected by the horizontal load.

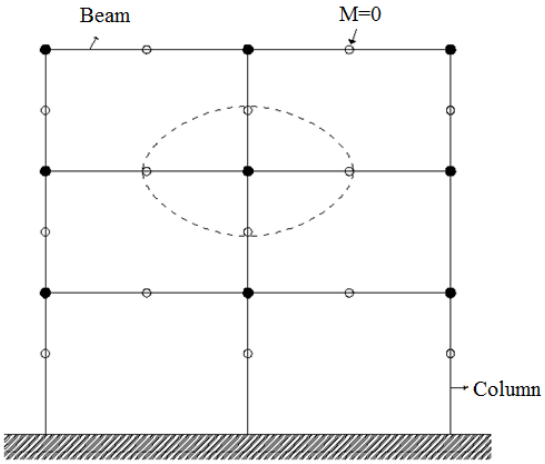

Figure 2. The interior beam-to-column joint in a moment resisting frame (represented in oval section)

3. EXPERIMENTAL ANALYSIS

Two large-scale, interior beam-column connection samples were prepared for testing. Reinforced concrete beam-column joint was used as control sample. Column and beam were regular reinforced concrete members designed according to local building codes. Engineered joint consist of two different parts: concrete encased steel composite part (the column) and reinforced

concrete part (the beam). The reinforced concrete beam was designed according to local design codes. The concrete encased steel composite column was designed according to EUROCODE 4 [22]. Details of the samples are given in following sections. As steel profile, IPE100 with 55mm flange was used. The foot of the column and end of the beams were pinned, thus, the boundary conditions were granted as it was given in Fig. 2. The column was loaded constant 200kN axial compression load that is approximately 10% of axial load capacity of the column. The sample was tested under cyclic loading. Loading was deformation controlled.

3.1. Geometry of the model and material properties

In both samples, the beams and columns are 20x20cm in cross section. Length of the beam is 260cm, length of the column is 180cm. The joint considered RC model is reinforced concrete beam-to-column joint. The joint dimensions and reinforcement detail is given in Fig. 3 and Fig. 4, and the material properties used in the numerical analysis are given in Table 1.

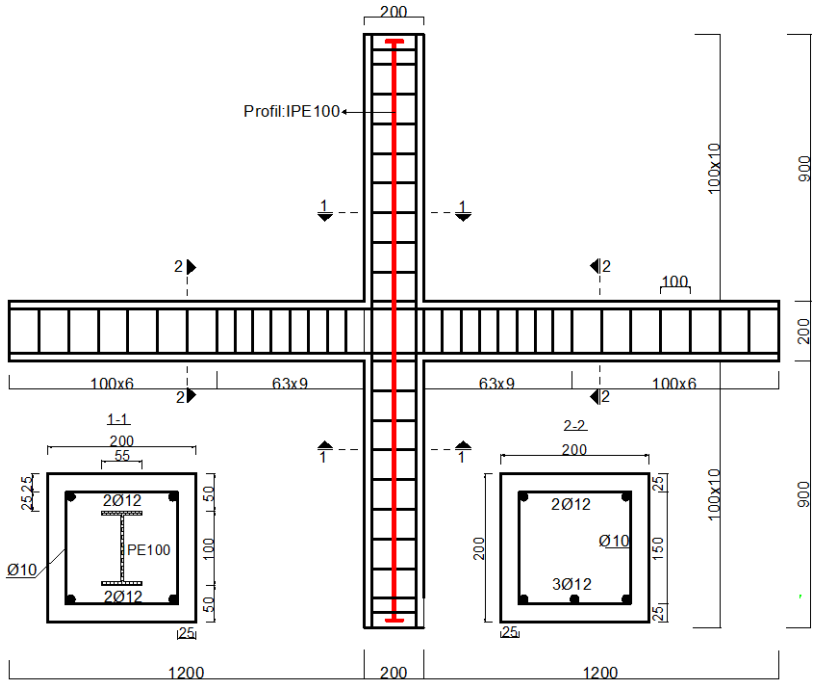

Figure 3. Dimensions and reinforcing detail of the cased steel composite column to reinforced concrete beam joint (SAMPLE 1)

Table 1. Material Properties

	Compressive Strength (MPa)	Yielding Strength (MPa)	Density (kg/m^3)	Modulus of Elasticity (GPa)	Poisson Ratio
Concrete	39		2400	34	0.2
Steel Profile	420	420	7850	200	0.3
Reinforcement	420	420	7850	200	0.3

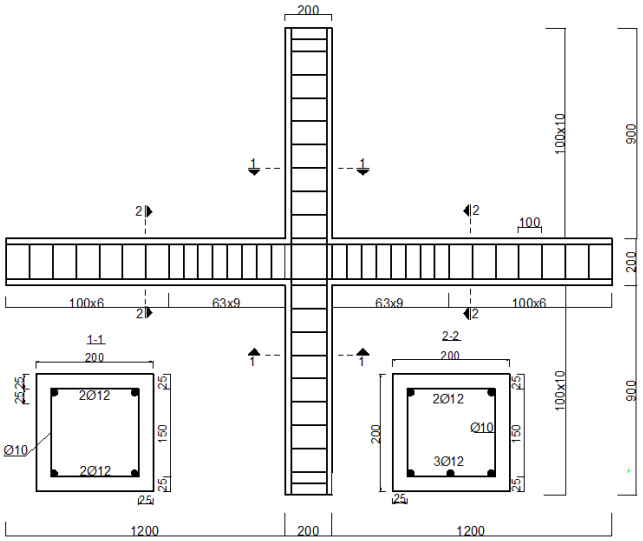

Figure 4. Dimensions and reinforcing detail of the reinforced concrete column-beam joint (SAMPLE 2)

3.2. Loading configuration and boundary conditions

The joint is numerically analysed under cyclic and axial compressive loading. The cyclic load is applied to the column horizontally at top end point, and the column is under effect of axial compressive load. The joint is supported from three points. The beam is supported from end points, and vertical movement of the beam is prevented. The loading configuration and supporting are shown in Fig.5 (P is cyclic loading representing earthquake effects; N is constant axial compressive load, representing internal axial loads). The load cycle applied is given in Fig. 6. The constant axial compressive load is 200kN, determined as 10% of the composite column compressive load capacity. Under cyclic and axial loading, the idealized deflection of the plane joint is shown in Fig. 7.

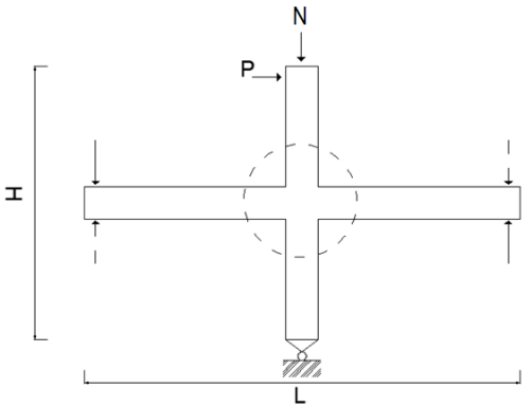

Figure 5. Loading configuration and boundary conditions of the joint, P is horizontal cyclic loading; N is constant axial compressive loading

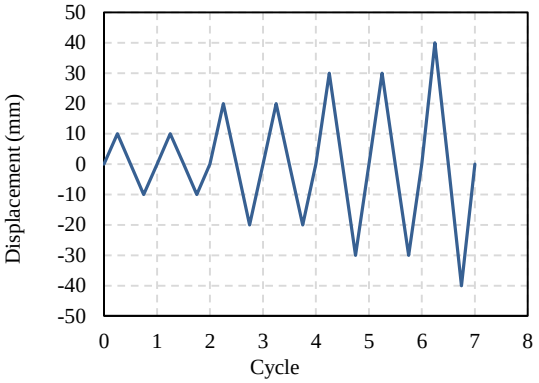

Figure 6. Repeated hysterical load cycle

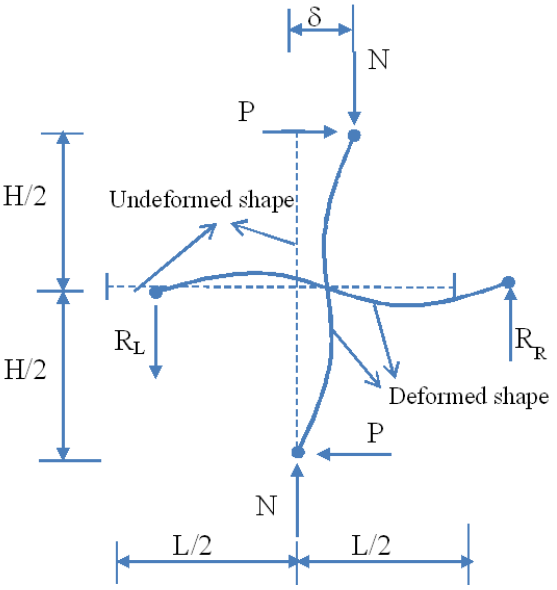

Figure 7. Deflected shape of idealized beam-to-column joint

Cyclic loading provides reverse repeated actions on the beam-column joints transmitted by the connected members. Simple mechanical approaches for the structural behaviour of the joint under effect of bending moment, axial and shear forces are expressed in many studies [23-24-25-26-27-28-29-30]. The strength capacity of the joint depends on the joint type, retrofitting, confinement, anchorage details, longitudinal reinforcements and steel core. In the proposed model, the steel core located in the column has ability to absorb shear forces. On the other hand, damage in the concrete cover would not be prevented. The fracture occurs in concrete at intersection of the column and beam followed by the yielding of the reinforcement. Since the loading is cyclic, the fracture starts where the tension is effective, later; it progress until failure of the joint. Representative deformation of the joint panel is shown in Fig. 8.

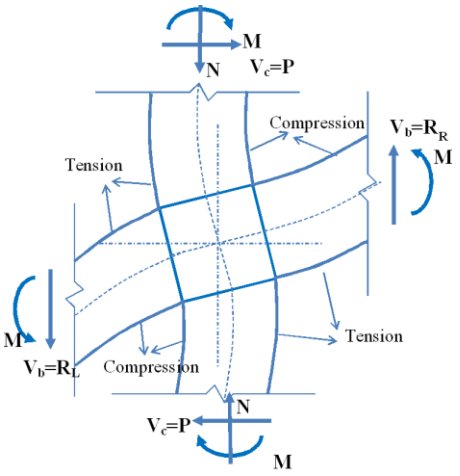

Figure 8. Idealized joint panel deformation

In the proposed joint, since the column contains steel profile, deformation of the joint panel would be same as the Fig. 8, however, the load transferring mechanism of the joint panel would contain web of steel profile and concrete panel as shown in Fig. 9. The joint panel is subjected to complex stress distributions due to bending moment, axial and shears forces. During stress transferring, the concrete under compression would crash, concrete under tension would crack. The failure would be controlled by the strength of the beam section. In order to exhibit true stress transferring, modelling of the joint should be carefully performed.

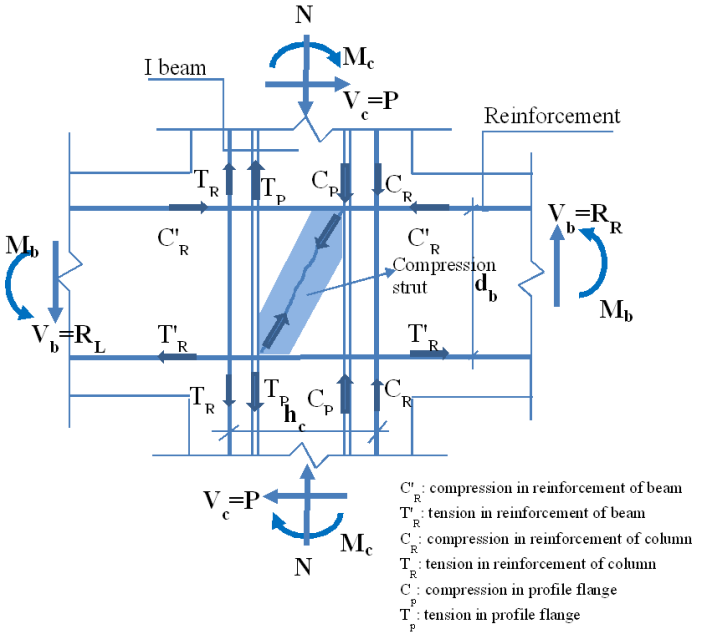

Figure 9. The joint panel a) steel web panel mechanism, b) concrete panel mechanism

In the core of the joint represented in Fig. 9, the internal loads transferred by concrete would be carried by both web of the steel profile and flanges while the moments effect at strong axis of column, carried by the flanges of the steel profile while the moments effect at weak axis. The local buckling at core panel would be prevented by concrete confinement delaying yielding of steel profile web.

3.3. Experimental setup, instrumentation and test procedure

The view of the test set-up and loading system is shown in Figure 10. Cyclic horizontal load was applied at the top of the column simulating seismic loading. During loading, each load cycle repeated twice to emphasize effect of certain load. The horizontal actuator is a servo controlled actuator and has a capacity of 500 kN with a 250mm stroke. The cyclic horizontal forces P (see Fig. 5) were considered as positive when it was from left to right, and negative when it was reversed, thus, compression tension regions were to be as represented as in Figure 8. The column was under effect of 200 kN constant axial compression simulating gravity loads. The displacements were measured from five different points, shown in Fig. 10. The strain measurements were made both from steel profile and reinforcing from multiple locations. The location of the strain gouges are given in Fig. 11.

Figure 10. Testing set up, loading system and location of potentiometers (D's are potentiometers)

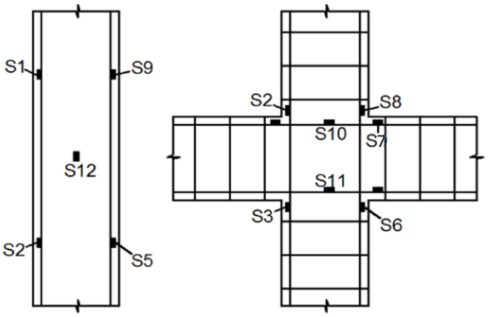

Figure 11. The location of the strain gouges both in steel profile and reinforcing

3.4. Experimental results and discussion

The performance of the specimens was evaluated through the measured strains and displacement data. Load-displacement measurements were collected, and damages and crack patterns were studied.

3.4.1. Concrete-encased steel composite column to RC beam joint (SAMPLE 1)

The cracks development of this specimen was observed during testing. The cracks were developed at the beam, and then they progressed to the joint panel shown in Fig. 12. Yielding occurred at fourth load cycle, about 17.67kN load at the beam where the tension occurs, and failure occurred at sixth load cycle about 29.41kN. Later on, when the loading continued, the cracks developed rapidly until the beam fractured, some of the cracks progressed to the joint panel, the joint exhibited "strong column-weaker beam design concept".

The specimen exhibited tensile damage at tension sides of beam, then, when loading continued, the beams fractured and diagonal concrete tensile damage progressed to the joint panel. When the load applied left to right, top of left side beam, bottom of right side beam and left flange of the I shape steel profile in the column was subjected to tension. When direction of the load reversed, the locations mentioned above became effect of compression. This repeated damages caused section fracture followed by yielding of the reinforcing in the beam. No yielding of I steel beam in column, and no compressive damage in the joint panel were observed. Diagonal tension cracking of the joint rapidly spread to the vicinity of the column.

Figure 12. Crack development in SAMPLE1

The load-displacement curve of the specimen is given in Fig. 13. There, the load versus displacement collected at D5 potentiometer is presented.

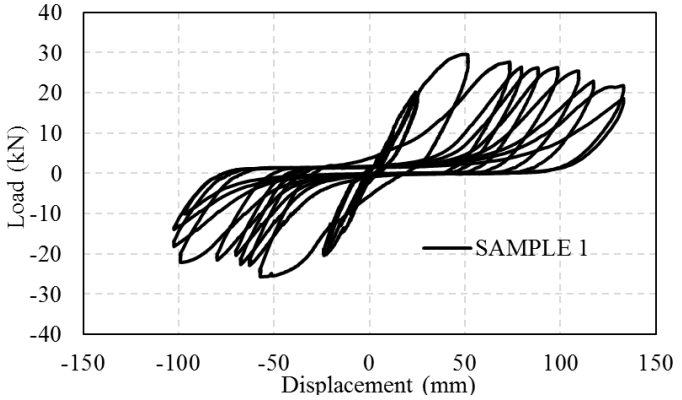

Figure 13. Load-displacement curve of concrete encased steel composite column-reinforced concrete beam joint (SAMPLE 1)

3.4.2. Reinforced concrete beam-column joint (SAMPLE 2)

In this sample again, cracks were developed at the beam, and then they progressed to the joint panel shown in Fig.14. Only, yielding occurred at third load cycle, about 17.42kN, and failure occurred at fifth load cycle about 27.83kN, then the cracks moved to joint panel and fracture occurred in joint panel indicating the design of the joint was improper. The load-displacement curve of the specimen is given in Fig. 15. There, the load versus displacement collected at D5 potentiometer is presented.

Figure 14. Crack development in SAMPLE 2

Initial response of the specimen was similar to SAMPLE 1. On the other hand, initial concrete shear damage was developed in joint panel fallowed by yielding of the column and beam longitudinal reinforcement in the joint panel zone. No yielding of I steel beam in column was observed.

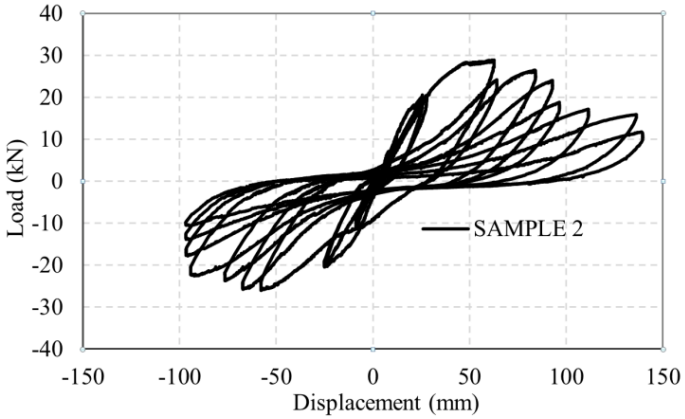

Figure 15. Load-displacement curve of concrete encased steel composite column-reinforced concrete beam joint for SAMPLE 2

When the graphics were reviewed, it is seen that cyclic behavior of the both specimens exhibited ductile behavior; on the other hand, engineered joint did not provide expected stiffness/load carrying capacity. The hysterical response of two specimens may be compared by envelop curves of responses shown in Fig. 16 better. As it seen, the capacity of the specimens is controlled by capacity of the beam. On the other hand, while SAMPLE 2 was reached failure, SAMPLE 1 exhibited longer ductility platform. The envelop load versus displacement relationships of the joint specimens were obtained by connecting the peak point of loading cycle on the hysteretic response graphics.

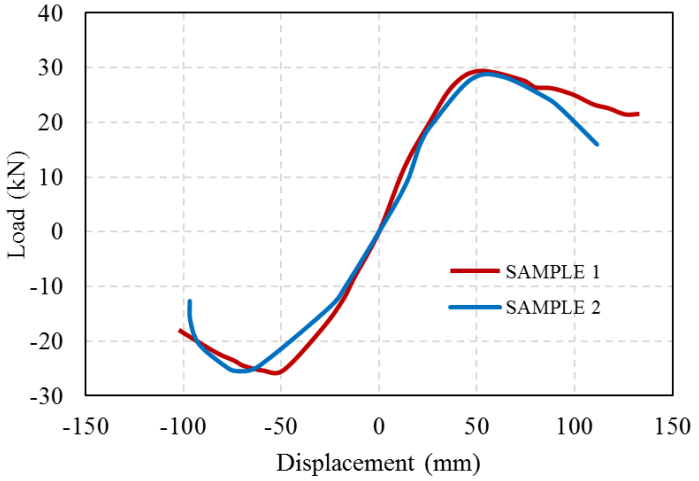

Figure 16. The envelope curves of the hysterical response of the specimens

Strain behaviour of the joints was observed in many locations, on the other hand only one location measurement presented here. The strain presented was measured on the reinforcement in the beam with strain gouge numbered S7, the location of it is also shown in the graphics, for both of the specimens. The horizontal load-strain graphics given in Fig. 17 and 18, for SAMPLE 1 and SAMPLE 2, respectively, expressed that the concrete encased steel composite column carried much of the strain in the joint, yet the beam fractured before the column taking the load.

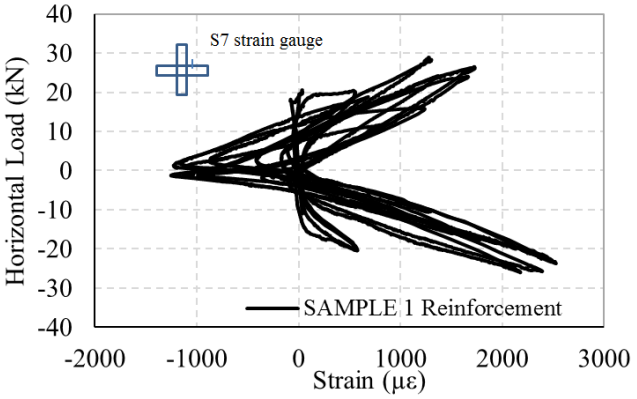

Figure 17. Strain response of the upper side reinforcement of the beam for SAMPLE 1

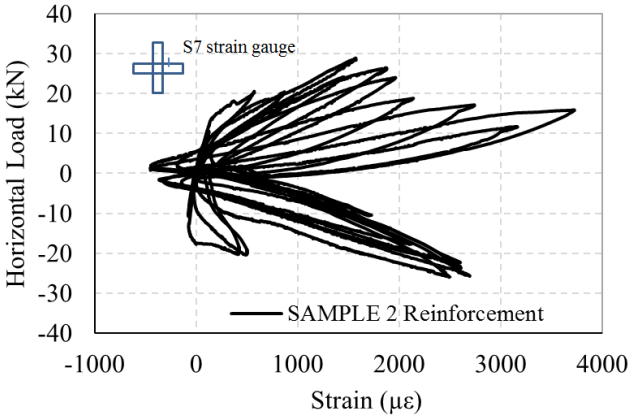

Figure 18. Strain response of the upper side reinforcement of the beam for SAMPLE 2

Table 1 presents the recorded loads at yielding (P_y), maximum (P_{max}) and failure (P_u) loads and corresponding displacements (Δ_y, Δ_{max}, Δ_u, yielding, max and ultimate, respectively).

Table 1. Load and displacement at different characteristic points.

	Yielding				Peak				Failure				
	P_y(kN)		Δ_y(mm)		P_{max}(kN)		Δ_{max}(mm)		P_u(kN)		Δ_u(mm)		μ
	(+)	(-)	(+)	(-)	(+)	(-)	(+)	(-)	(+)	(-)	(+)	(-)	
SAMPLE 1	17.67	15.85	21.56	19.12	29.41	-25.36	51.48	-48.99	21.57	-16.95	133.05	-102.37	6.16
SAMPLE 2	17.42	15.26	21.25	18.95	27.83	-24.66	46.84	-61.83	15.96	-12.7	111.41	-96.78	5.24

The maximum load P_{max}, maximum displacement Δ_{max}, ultimate load P_u, ultimate displacement Δ_u, and the ductility coefficient μ are obtained from the envelope load-displacement curve. The ductility coefficient is calculated by the Δ_u/Δ_y, and the yield displacement Δ_y is the calculated by the effective energy method [30].

4. STIFFNESS DEGRADATION

Reinforced concrete structural components will exhibit some level of stiffness degradation when subjected to reverse cyclic loading. Stiffness degradation is the result of cracking of the concrete. The level of stiffness degradation depends on the material properties, geometry and ductility level of the components, and loading history. As long as, the structural components crack, stiffness degradation should be expected. On the other hand, stiffness degradation is to be in between cycles rather than in-cycle. The models analysed exhibited stiffness degradation as shown in Fig 19. The differences that are not observed at load-displacement response between SAMPLE 1 and SAMPLE 2 are observed at stiffness degradation graphic. It is noted that SAMPLE 1 has larger stiffness capacity than SAMPLE 2.

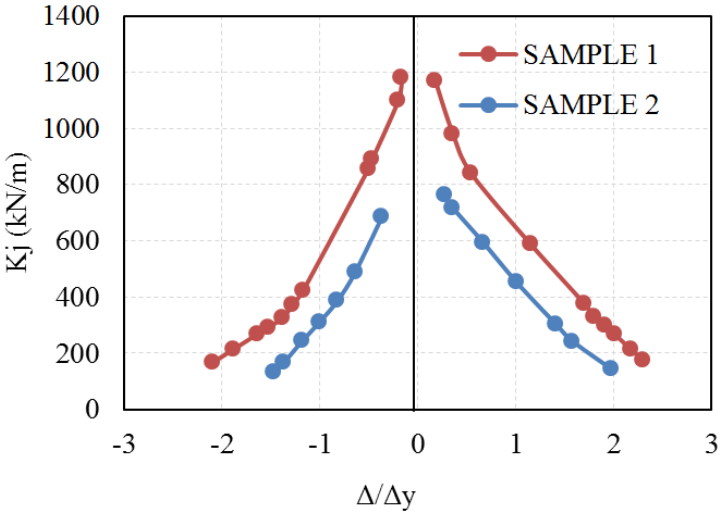

Figure 19. Stiffness- Δ/Δ_y relation

5. FINITE ELEMENT MODELING

Analytical Finite Element model was implemented in ABAQUS/Standard module. Non-linear analysis of the all type of joints was performed in ABAQUS program.

Modelling of members was made using suitable elements according to manual. Concrete was modeled as solid, C3D8R type element. In all models, 1408 numbers of elements were used for concrete. Steel profile was modeled as beam, using B31 type, 39 numbers of elements were used. Reinforcing bars were modeled as truss member, using 2632 numbers of T3D2 elements. The bonding between concrete and steel beam was constituted by using surface-to-surface contact approach, as explained in ABAQUS program documentation to ensure fully-composite beam model.

The ABAQUS uses Concrete Damage Plasticity (CDP) model to simulate inelastic behavior of the concrete. The model is suitable for reinforced concrete as well as plain concrete.

Furthermore, the model is capable to describe the irreversible damage that occurs during the fracturing process in concrete subjected to monotonic, cyclic, and/or dynamic loading under low confining pressures. The model assumes that two main failure mechanisms are tensile cracking and compressive crushing of the concrete material. Stress-strain curve for concrete in order to use CDP model in ABAQUS was gathered by material testing and it is given in Fig. 20.

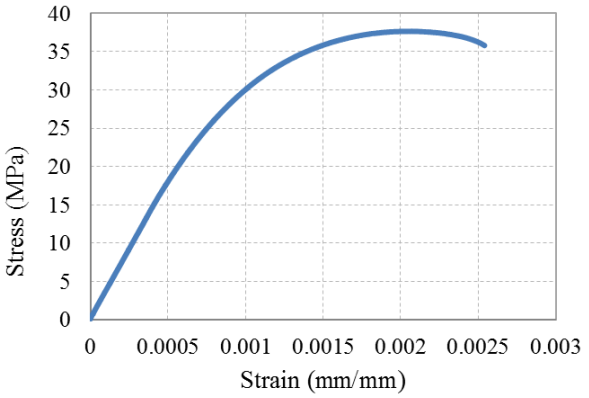

Figure 20. Stress-strain curve of the concrete used in analysis

Modelling of the specimens are given in Fig. 21.

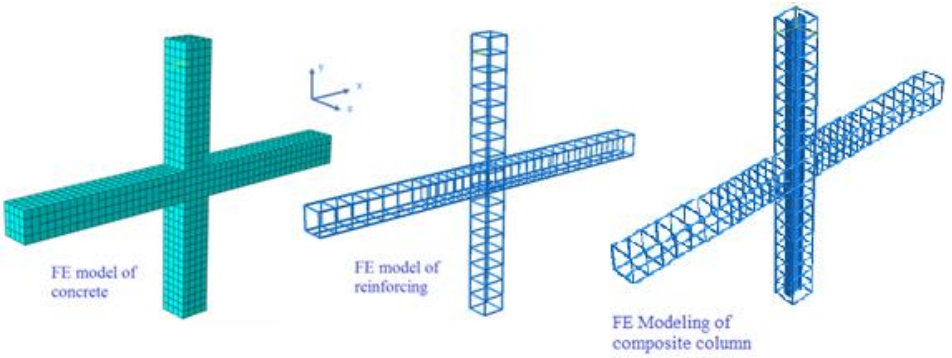

Figure 21. FE modeling of the samples: given separately for concrete, reinforcing and reinforcing and steel profile

Numerical analysis results of the joints under horizontal cyclic loading are given as principal stress distributions for concrete encased steel column-RC beam joint (SAMPLE 1) in Fig. 22, for reinforced concrete beam-column joint (SAMPLE 2) in Fig.23.

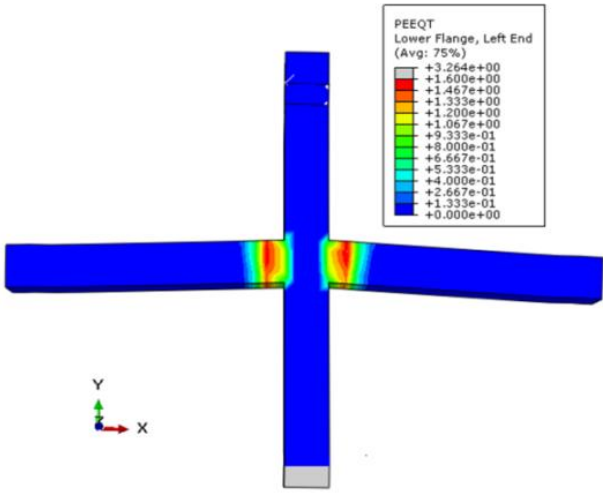

Figure 22. Principal stress contours in concrete for concrete encased steel column-RC beam (SAMPLE 1)

Principal stress image given in Fig. 22 shows that the capacity of the joint is governed by the capacity of the beam. The failure occurred in beam at column surface. On the other hand, in reinforced concrete beam-column joint (SAMPLE 2) the failure occurred in the joint panel, as shown in Fig. 23.

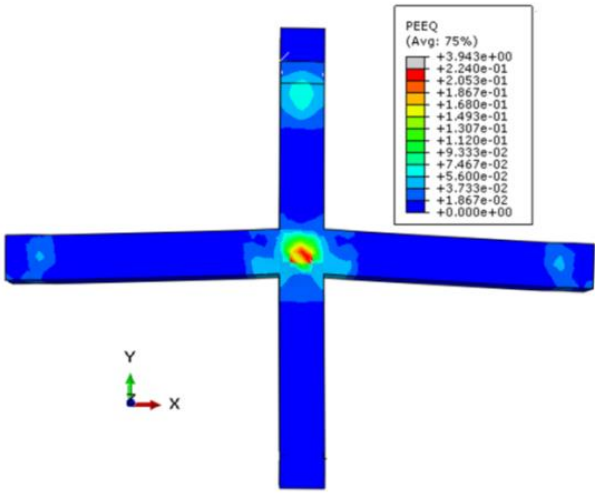

Figure 23. Principal stress contours in concrete for concrete encased steel column-RC beam (SAMPLE 2)

Comparison of the numerical and experimental analysis results is given in Fig. 24. Although, numerical analysis results exhibited slightly larger capacity and ductility than actual behaviour (regarding experimental results), the differences may be considered in acceptable limits.

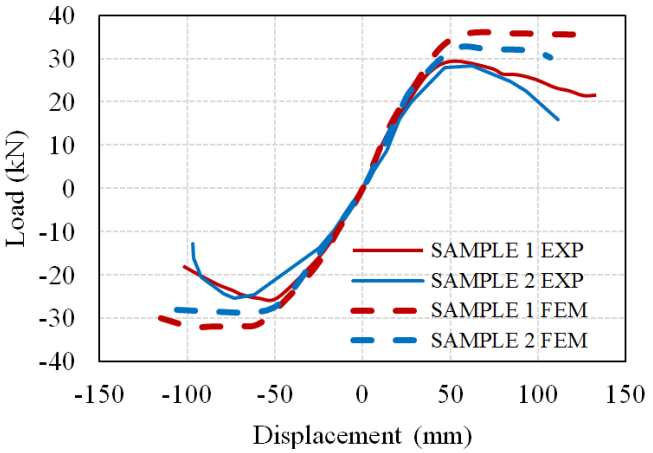

Figure 24. The envelope curves of the hysterical response of the specimens in numerical and experimental analysis

6. CONCLUSION

Experimental and numerical analysis of the concrete encased steel profile composite column-to reinforced concrete beam and reinforced concrete column-to beam joints under cyclic loading are presented.

Analyses are completed in both in numerical and experimental. Numerical analysis results are verified by experimental analysis. Results indicated that both joints exhibited same load carrying capacity, yet, the fracture occurrence was different. In addition to that, analysis result showed that the failure controlled by behavior of the beam and joint capacity was depended on the shear capacity of the beam. Although stress concentration was located at centre of the joint, the failure induced by concrete crashing, both in column and beam.

Response of the joint is presented via load-displacement curves and stiffness degradation. Because of the failure controlled by beam capacity, the load-displacement responses of both joints are similar. On the other hand, energy dissipated by joints is different, as it is observed from stiffness degradation.

In numerical analysis, progressive crack occurrence (active yielding) was also studied; results are exhibited for SAMPLE 1 and SAMPLE 2 in Fig. 25 and 26, respectively. The images given in Fig. 25 and 26 are contains crack in concrete and yielding in steel. The red cells are indicating failed (implying cracks) FE members under load. The loads indicated at the top of the images beside displacements are the load at the moment the images were taken. The arrows indicate the direction of the load. Thus the crack propagation in the models may be seen from images for different loads cycles. The crack pattern at the images given in Fig. 25 and 26 closely resembles the crack pattern observed in experimental study as shown in Fig. 12 for SAMPLE 1, in Fig. 14 for SAMPLE 2, respectively.

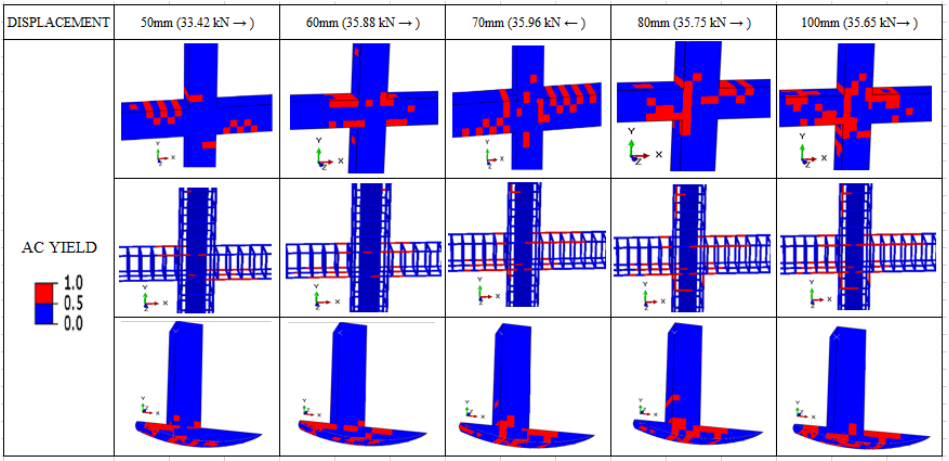

Figure 25. Active yielding pattern of SAMPLE 1 (images in first line indicate the cracks in concrete, in second line indicate yielding in reinforcement, third line indicate crack locations in joint cross section)

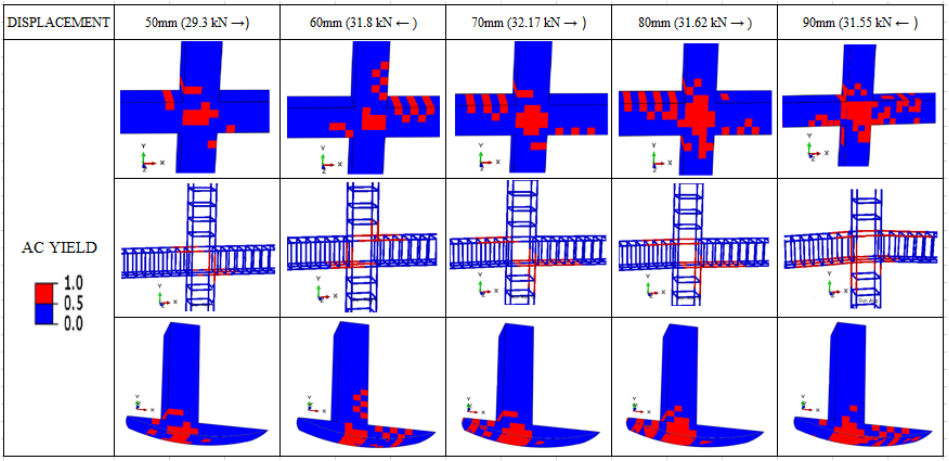

Figure 26. Active yielding pattern of SAMPLE 2 (images in first line indicate the cracks in concrete, in second line indicate yielding in reinforcement, third line indicate crack locations in joint cross section)

REFERENCES

[1] Lee, S. J. Seismic behavior of steel building structures with composite slabs. Thesis resented to Lehigh University at Bethlehem, Pa, in partial fulfillment of the requirements for the degree of Doctor of Philosophy, (1987).

[2] Lee S-J, Lu L-W. a. Cyclic tests of full-scale composite joint sub assemblages. J Struct Eng, ASCE 1989(8):1977–98.

[3] Lee, S.-J., Lu, L.-W., Cyclic load analysis of composite connection sub assemblages. In: Connections in steel structures II, Eds: Bjorhovde, Colson, Hajjar, Stark, AISC, Pittsburgh. pp. 209-216.

[4] J. Fan, Q. Li, J. Nie, and H. Zhou, "Experimental study on the seismic performance of 3D joints between concrete-filled square steel tubular columns and composite beams," Journal of Structural Engineering, vol. 140, no. 12, Article ID 04014094, 2014.

[5] Zeng L, Cui Z, Xiao Y, Jin S, and Wu Y. Cyclical Behavior of Concrete-Encased Composite Frame Joints with High Strength Concrete. Hindawi Publishing Corporation 2015; Article ID 873162.

[7] Liao FY, Han LH, Tao Z. Behavior of composite joints with concrete encased CFST columns under cyclic loading: Experiments. Engineering Structures 2014; 59: 745–764.

[8] Chen CC, Chen Chien C, Hoang TT. Role of concrete confinement of wide-flange structural steel shape in steel reinforced concrete columns under cyclic loading. Engineering Structures 2016; 110 : 79–87.

[9] Weng, C.C., Yen, S.I. Comparisons of concrete-encased composite column strength provisions of ACI code and AISC specification. Engineering Structures, 2002; 24: 59–72.

[10] Di Sarno, L., Pecce, M.R., Fabbrocino, G. Inelastic response of composite steel and concrete base column connections. Journal of Constructional Steel Research, 2007; 6:3 819–832.

[11] Ellobody, E., Young, B. Numerical simulation of concrete encased steel composite columns. Journal of Constructional Steel Research, 2011; 67:211–222.

[12] Begum M, Driver, R.G. Elwi, A.E. Behaviour of partially encased composite columns with high strength Concrete. Engineering Structures, 2013, 56: 1718–1727.

[13] Nzabonimpa, J.D. Hong W-K., Jisoon, K. Nonlinear finite element model for the novel mechanical beam-column joints of precast concrete-based frames, Computers and Structures, 2017, 189:31–48.

[14] Ouyang,Y., Kwan, A.K.H., Lo, S.H., Ho, J.C.M. Finite element analysis of concrete-filled steel tube (CFST) columns with circular sections under eccentric load, Engineering Structures, 2017, 148:387–398.

[15] Salem, A.S., Taleb, S.A., Tahar, K.A. Static and dynamic behavior of composite concrete-based beams with embedded polymer/FRP components. Procedia Engineering, 2015, 114:173 – 180.

[16] Wang, K., Lu, X-F., Yuan, S-F., Cao, D-F., Chen-X. Analysis on hysteretic behavior of composite frames with concrete-encased CFST columns. Journal of Constructional Steel Research, 2017, 135:176–186.

[17] Carrera, E., Zappino, E., Li, G. Finite element models with node-dependent kinematics for the analysis of composite beam structures. Composites Part B, 2018, 132:35-48.

[18] Weng, C.C., Yen, S.I. Comparisons of concrete-encased composite column strength provisions of ACI code and AISC specification, Engineering Structures, 2002; 24: 59–72.

[19] Di Sarno, L., Pecce, M.R., Fabbrocino, G. Inelastic response of composite steel and concrete base column connections. Journal of Constructional Steel Research, 2007; 6:3 819–832.

[20] Gonçalves, R., Carvalho, J. An efficient geometrically exact beam element for composite columns and its application to concrete encased steel I-sections. Engineering Structures, 2014; 75:213–224.

[21] ABAQUS (2005), Finite Element Modeling Software, Rhode Island, USA.

[22] Eurocode 4 : Design of composite steel and concrete structures Part-1 : general rules and rules for buildings. Brussels: European committee for Standardization; 2005

[23] ACI 318-83 (1986), Building Code Requirements For Reinforced Concrete, American Concrete Institute; Farmington Hills, MI, USA.

[24] Yu-Feng An, Lin-Hai Han, Roeder, C. Performance of concrete-encased CFST box stub columns under axial compression, Structures 3 (2015) 211–226.

[25] Paulay T. and Priestley, M. J. N. Seismic design of Reinforced Concrete and masonry buildings.. John Wiley & Sons, Inc., 1992, p. 744.

[26] Birely, A.C., Lowes, L.N., Lehman, D.E. A model for the practical nonlinear analysis of reinforced-concrete frames including joint flexibility. Engineering Structures, 2012; 34:455–465.

[27] Song, T-Y., Han, L-H., Zhong, T. Performance of Steel-Reinforced Concrete Beam-to-Column Joints after Exposure to Fire. J. Struct. Eng., 2016, 142(10): 04016070

[28] Pantelides, C.P., Okahashi, Y., Reaveley L. D. Seismic Rehabilitation of Reinforced Concrete Frame Interior Beam-Column Joints with FRP Composites. J. Compos. Constr., 2008, 12(4): 435-445.

[29] Okahashi, Y., Pantelides, J.P. Str ut-and-tie model for interior RC beam-column joints with substandard details retrofitted with CFRP jackets. Composite Structures, 2017; 165:1–8

[30] Del Vecchio, C., Di Ludovico, M., Prota, A., Manfredi, G. Analytical model and design approach for FRP strengthening of non-conforming RC corner beam–column joints. Engineering Structures, 2015; 87: 8–20.